DOI: 10.18462/iir.gl.2018.1286

COMPARISON OF RANKINE CYCLE AND TRILATERAL FLASH CYCLE FOR POWER PRODUCTION FROM LOW TEMPERATURE HEAT SOURCES

Daniel Rohde[(a)], Brede A.L. Hagen[(a)], Stian Trædal[(a)], Trond Andresen[(a)]

[(a)] SINTEF Energy Research

Trondheim, 7465, Norway, daniel.rohde@sintef.no

ABSTRACT

The performance of the Rankine Cycle (RC) and the Trilateral Flash Cycle (TFC) were compared for power production from sensible low temperature heat sources. Air was chosen as heat source fluid with a mass flow of 10 kg/s and temperatures of 100, 150, and 200°C. Water was chosen as heat sink with a temperature of 20°C. Butane, isopentane, and propane were chosen as natural working fluids and were compared to three commonly used HFO/HFCs as benchmark. The power cycles were optimized for maximum net power for a limited total heat exchanger area, and with a variable efficiency for the TFC's two-phase expander. The TFC reached higher maximum power outputs than the RC for the 100°C case. However, the required heat exchanger area and expander outlet volume flow rate were significantly higher for the TFC, indicating a larger and more expensive system. The differences in system size and performance decreased for the higher heat source inlet temperatures. The natural working fluids showed similar performance compared to the benchmark refrigerants.

Keywords: Rankine Cycle, Trilateral Flash Cycle, Heat-to-Power Conversion, Natural Working Fluids

1. INTRODUCTION

The world's energy demand is rising, leading to increasing emission of greenhouse gases such as CO_2. It is therefore necessary to search for alternative energy sources and improve existing methods for power production. In this study, the possibility of improving power production from low temperature waste heat sources by using the Trilateral Flash Cycle (TFC) instead of the standard Rankine Cycle (RC) was investigated. Temperature-entropy diagrams of both cycles are shown in Fig. 1.

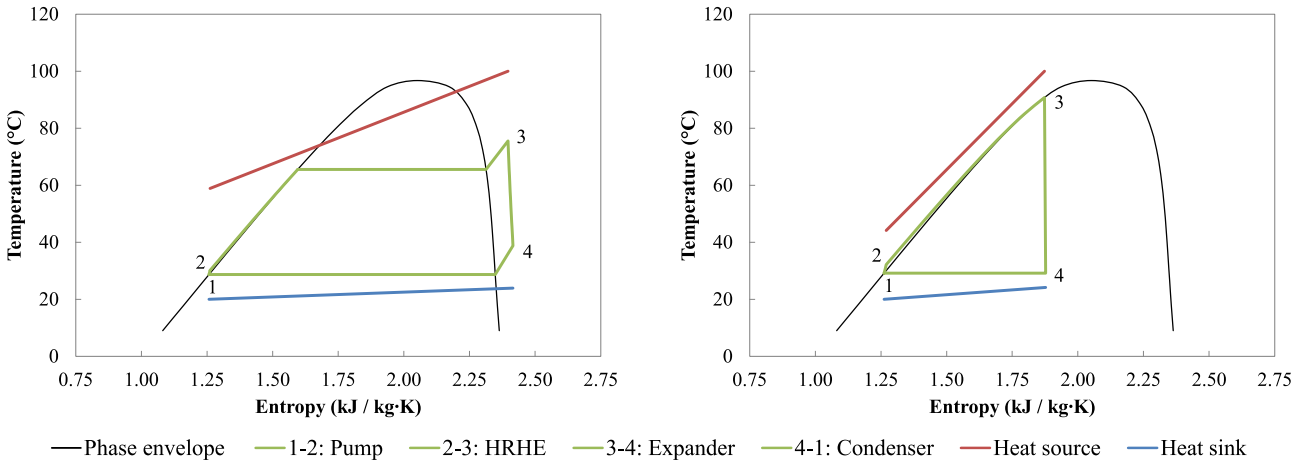

Figure 1. T,s-diagrams of RC (left) and TFC (right) with propane as working fluid.

The RC is a well-established technology for power production from low to medium temperature heat sources. Common applications range from waste heat to solar and geothermal power plants (Quoilin *et al.*, 2013). A known drawback of the RC from a thermodynamic point of view is the suboptimal temperature matching in the heat recovery heat exchanger (HRHE) for sensible heat sources. This is a result of the constant evaporation

DOI: 10.18462/iir.gl.2018.1286

temperature of the working fluid and the cause of significant exergy losses (Galanis *et al.*, 2009). To improve the temperature matching, the use of zeotropic working fluid mixtures or supercritical pressures has been suggested to transfer the heat at a gliding and thus better temperature profile. However, an optimal temperature match is only obtained when both fluids are in liquid phase so that the temperature difference in the heat exchanger is almost constant (DiPippo, 2007). This is the case for the TFC as can be seen in Fig. 1. The expansion process is therefore entirely different for the two power cycles. While an RC has its expansion in the superheated vapor region, a TFC expands into the two-phase region (3-4 in Fig. 1), resulting in flash evaporation of the working fluid (giving the TFC its name). This leads to much higher volume ratios between inlet and outlet than for dry vapor expanders and makes the flow characteristics harder to predict. Turbines and expanders commonly used in RCs do not tolerate liquids or even liquid droplets, so this two-phase expansion requires specially designed expanders.

A few expander types tolerate two-phase flow. For small-scale (1-10 kW) applications, scroll or rotary vane expanders can be used (Bao and Zhao, 2013). For slightly larger systems, a reciprocating piston might be suitable. However, since the piston itself does not tolerate two-phase flow, it can only be used as expander in a TFC when a cyclone for phase separation is implemented upstream (Steffen *et al.*, 2013). For medium-scale (50-250 kW) systems as investigated in this study, screw expanders and the Variable Phase Turbine (VPT) are the most relevant expander types. A screw expander is a positive displacement expander that consists of a pair of meshing helical rotors in a casing. The volume trapped between the rotors and the casing changes as the rotors rotate. The energy transfer between the fluid and the rotor depends mainly on the pressure on the rotors and only to a small extent on the dynamic effects of fluid motion. This is why the presence of liquid in the expander has little effect on its mode of operation or efficiency (Smith *et al.* (1994), Smith *et al.* (2005)). The VPT consists of a set of individual fixed nozzles and an axial impulse rotor. In the nozzles, the working fluid's enthalpy is partly converted to kinetic energy in a near isentropic expansion. The inlet to the nozzle can be liquid, two-phase fluid, supercritical fluid, or vapor. The kinetic energy of the two-phase jets is converted to shaft power in an axial impulse turbine that allows direct driving of a generator, so no gearbox and lube oil systems are needed (Welch and Boyle, 2009).

The TFC was originally developed for geothermal applications and was investigated as far back as 1989 (Hu *et al.*, 1989). The first publications describing the TFC in detail are from Smith and indicate great potential for geothermal applications (Smith, 1993). Smith *et al.* (1995) focused on the implementation of screw expanders and indicated cost-advantages of TFC systems with screw expanders compared to commonly used RC systems with dry vapor turbines. However, no reports of commercial applications could be found. Brown and Mines (1998) performed a fluid study for the TFC with 20 working fluids and analyzed two different inlet temperatures of the heat source, which were set to 93°C and 160°C. They compared the cycle performance of an RC with isobutane to a TFC with n-pentane as working fluids and found that the TFC can give higher power output for equal expander efficiencies, but only at larger heat exchanger area. They mention that the two-phase expansion would very likely be less efficient and showed that it would need to be at least 0.76 to match the performance of the RC. Yari *et al.* (2015) compared TFC to a Kalina cycle and an RC for a heat source of 120°C, and concluded that TFC could produce more power than the Kalina cycle or the RC, but this depended very much on the isentropic efficiency of the two-phase expander.

2. METHODOLOGY

To compare the performance of RC and TFC, both cycles were simulated with a model developed in Microsoft Excel using REFPROP 9 (Lemmon *et al.*, 2013) for the calculation of thermodynamic properties. Parts of the model have been described by Trædal *et al.* (2014), but are repeated here for the sake of completeness.

2.1 Cycle Calculation and Optimization

Table 1 lists the main parameters and variables that were used during the calculations. The cycles were calculated based on energy balances with a number of constraints to avoid unfeasible solutions. The minimum temperature difference (pinch point) in the heat exchangers was set to 1 K to avoid unrealistic temperature profiles. The minimum superheat at the outlet of the heat recovery heat exchanger for the RC was also set to 1 K. The pump outlet pressure was limited to 95% of the working fluid's critical pressure and the condensation pressure was kept above one bar to avoid a sub-atmospheric system.

DOI: 10.18462/iir.gl.2018.1286

Table 1. Calculation parameters and variables.

Description	Type/Value	Description	Type/Value
Cycle		**Heat recovery heat exchanger**	
Heat loss to ambient	Neglected	Pressure drops	Neglected
Tot. heat exchanger area	500/1000/1500/2000/2500 m²	U heater	90 W/(m²·K)
Efficiency	Result	U evaporator (RC)	100 W/(m²·K)
Net power output	Optim. target, see Eq. (1)	U superheater (RC)	50 W/(m²·K)
Pump		Degrees superheat (RC)	Optim. variable
Mass flow working fluid	Optim. variable	Min. pinch point	1 K
Isentropic efficiency	0.70	Area	Result
Motor efficiency	0.90	**Condenser**	
Inlet pressure	Result	Condensation temperature	Optim. variable
Outlet pressure	Optim. variable	Pressure drop working fluid	Neglected
Work	Result	Pressure drop heat sink	100 kPa
Expander		U de-superheater	90 W/(m²·K)
Isentropic efficiency (RC)	0.80	U condenser	900 W/(m²·K)
Nozzle efficiency (TFC)	Result, see Eq. (3)	Min. pinch point	1 K
Rotor efficiency (TFC)	Result, see Eq. (4)	Area	Result
Generator efficiency	0.90	**Heat sink**	Water
Min. vapor fraction (RC)	100%	Mass flow	Result
Work	Result	Inlet temperature	20°C
Heat source	Air	Inlet pressure	3 bar
Mass flow	10 kg/s	Outlet temperature	Optim. variable
Inlet temperature	100/150/200°C	Pump efficiency	0.70
Inlet pressure	3 bar	Motor efficiency	0.90
Outlet temperature	Result	Pump work	Result

The following variables were optimization variables: Working fluid mass flow, pump outlet pressure, condensation temperature, heat sink outlet temperature, and superheat at expander inlet (RC only). These were optimized for each calculation to maximize the net power output. Using net power output as optimization target instead of cycle efficiency is recommended for sensible heat sources (Quoilin *et al.*, 2011). The net power output was defined as

$$P_{\text{net}} = P_{\text{expander}} \cdot \eta_{\text{generator}} - P_{\text{pumps}} / \eta_{\text{motor}} \quad (1)$$

with P_{pumps} being the sum of working fluid pump power and heat sink pump power. The Excel solver was used with the «Generalized Reduced Gradient Nonlinear» solving method with forward derivatives to perform the optimization. A high number of starting points was chosen to ensure that the global maximum was found with high probability.

To calculate the heat exchanger area (A), the log mean temperature difference (LMTD) was used. The heat recovery heat exchanger was divided into a heating, evaporating, and superheating section. The condenser was divided into a de-superheating and a condensing section. The heat transfer coefficients (U) were assumed to be constant for each section, see Table 1. They were set according to values presented in (Ho, 2012), where an order of magnitude approximation was used to define overall heat transfer coefficients for different stream combinations which were comparable to published values. The area for each section was thus calculated as

$$A = Q / (U \cdot \text{LMTD}) \quad (2)$$

with Q being the heat flow in the respective section of the heat exchanger.

DOI: 10.18462/iir.gl.2018.1286

All component efficiencies were assumed constant except for the expander efficiency of the TFC, see Table 1. The two-phase expander was modeled as a Variable Phase Turbine. The nozzle and rotor efficiencies were calculated separately. The nozzle efficiency was calculated as

$$\eta_{\text{nozzle}} = 0.865 + 0.00175 \cdot \rho_{4,\text{vapor}} \quad (3)$$

with $\rho_{4,\text{vapor}}$ being the vapor density at condensing pressure. The rotor efficiency was calculated as

$$\eta_{\text{rotor}} = 0.575 + 0.325 \cdot q_4 \quad (4)$$

with q_4 being the vapor quality at nozzle exit. These relationships are based on values in Welch and Boyle (2009), Hays (2010) and personal communication with the author of the latter (Hays, 2010). They allow a more realistic comparison between different working fluids, as the main influencing properties are taken into account. However, these simplified relationships are not validated and should thus only be used as indications.

2.2 Case Definition

Three hypothetical cases were defined, all using air as heat source fluid with a mass flow of 10 kg/s. The temperature of the air was set to 100, 150, and 200°C for Cases I, II, and III, respectively. Water at 20°C was chosen as heat sink for all cases. To analyze how power output changes with system size, the maximum total heat exchanger area was constrained during the optimization. All cases were calculated with five different constraint values spanning 500 to 2500 m². The maximum total heat exchanger area was the sum of all calculated sections: heater, evaporator, superheater, de-superheater and condenser. Pressure drops were neglected, except for the heat sink side of the condenser. Here, the pressure drop was needed to calculate the heat sink pump power, which influenced the optimization target (net power output).

2.3 Working Fluid Selection

Conventional fluids used in low temperature RC plants today are R134a and R245fa (Quoilin *et al.*, 2013) and were therefore chosen as reference. R1234ze(E) was added as it has received interest as a "new generation" of low-GWP (global warming potential) HFO-fluids (Zyhowski and Brown (2011), Li *et al.* (2017)). As promising natural working fluids, three hydrocarbons with different critical temperatures (T_{crit}) were chosen, see Table 2.

Table 2: Selected working fluids

Fluid	R134a	R245fa	R1234ze(E)	Propane	Butane	Isopentane
T_{crit} (°C)	101.1	154.0	109.4	96.7	152.0	187.2
GWP	1300	1030	6	20	20	20

3. RESULTS

The values for optimized net power production are shown in Fig. 2 to Fig. 4 for Cases I to III, respectively. The net power is plotted against total heat exchanger area and expander outlet volume flow as these values are expected to have the most influence on the total system costs. Increasing the constraint value for total heat exchanger area led to higher power output until the pinch point limitation of 1 K was reached in both heat exchangers. Additional simulation results are shown in Table 3 to Table 5 for Cases I to III, respectively.

For Case I, the power output of the TFC depended much more on the heat exchanger area than the power output of the RC. At 500 m², the RC performed significantly better, but the TFC reached higher power outputs above 1500 m². This was due to the pinch point limitation in the heat recovery heat exchanger, which limited the heat source utilization especially in the RC. The TFC reached lower heat source outlet temperatures, see Table 3. However, the expander outlet volume flows were also higher for the TFC.

The different working fluids showed very similar performance for the RC. The TFC showed slightly larger differences with propane yielding the lowest power output. R245fa and isopentane showed the highest power output but also the highest expander volume flows.

DOI: 10.18462/iir.gl.2018.1286

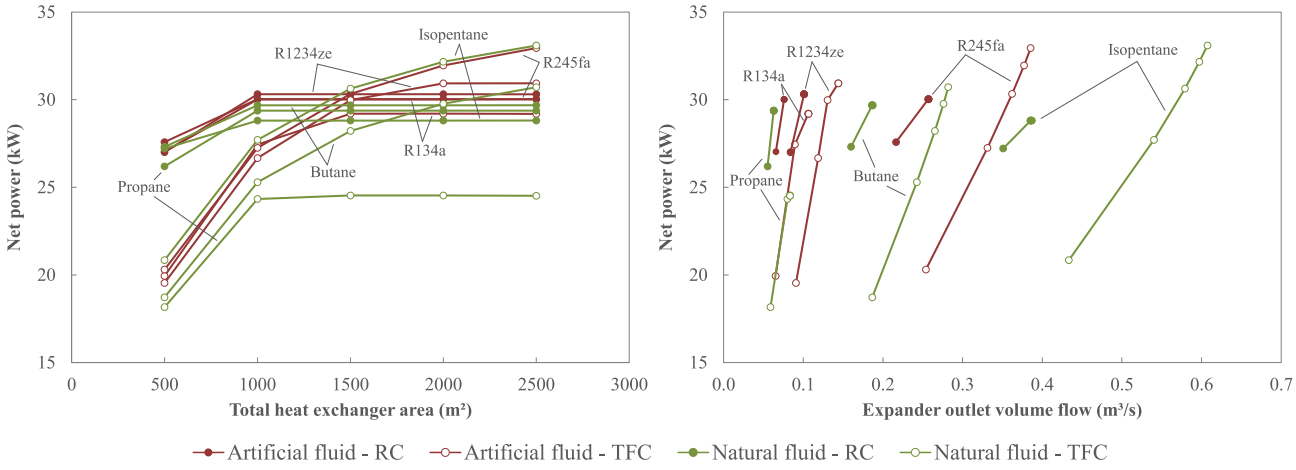

Figure 2. Net power plotted against system size indicators. Case I (heat source inlet temperature 100°C).

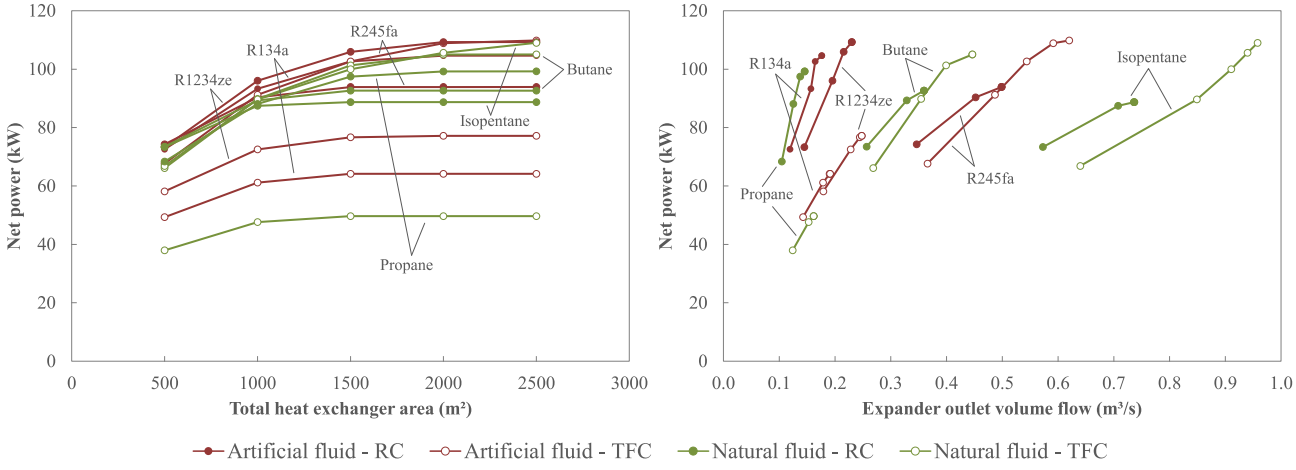

Figure 3. Net power plotted against system size indicators. Case II (heat source inlet temperature 150°C).

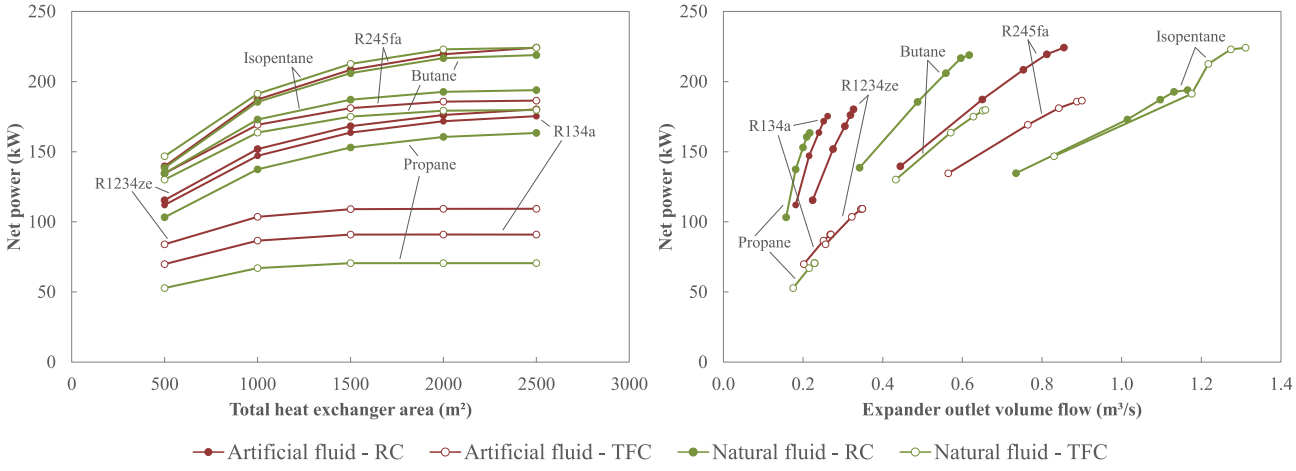

Figure 4. Net power plotted against system size indicators. Case III (heat source inlet temperature 200°C).

For Case II, the maximum power outputs were very similar for RC and TFC and around three times higher than for Case I. The expander volume flows were significantly lower for the RC and around twice as large as for Case I. The efficiency of the TFC expander increased compared to Case I. R134a, R1234ze, and propane

were shown to be unsuitable for a TFC due to their low critical temperature, which led to a large temperature difference at the HRHE inlet and thus a suboptimal temperature profile.

For Case III, the maximum power outputs of isopentane (TFC), R245fa (RC), and butane (RC) were almost the same and twice the size of Case II. As expected, expander volume flows were even higher than for Case II. The high-side pressure increased significantly for higher heat source temperatures (until the maximum value was reached). It was also generally higher for the TFC than for the RC, especially at lower heat source temperatures.

Table 3. Selected result details. Case I (100°C) with 1000 m².

Fluid	Cycle	Net power output	Working fluid pump power	Pump outlet pressure	Working fluid mass flow	Expander volume flow (out)	Expander efficiency	Heat source outlet temperature
		kW	kW	bar	kg/s	m³/s	-	°C
R134a	RC	30	3.7	19.2	2.2	0.08	0.80	53.2
	TFC	27	18.9	36.9	4.8	0.09	0.71	43.3
R245fa	RC	30	0.9	5.3	2.1	0.26	0.80	54.8
	TFC	27	7.3	11.2	6.3	0.33	0.64	39.8
R1234ze(E)	RC	30	3.4	14.7	2.6	0.10	0.80	52.1
	TFC	27	16.5	28.0	5.3	0.12	0.70	42.6
Butane	RC	30	1.4	7.2	1.1	0.19	0.80	54.9
	TFC	25	10.3	13.8	3.3	0.24	0.64	40.4
Isopentane	RC	29	0.6	3.1	1.1	0.39	0.80	56.3
	TFC	28	5.1	6.4	3.7	0.54	0.63	39.9
Propane	RC	29	5.3	23.8	1.2	0.06	0.80	53.3
	TFC	24	25.7	40.3	2.6	0.08	0.70	40.4

Table 4. Selected result details. Case II (150°C) with 1000 m².

Fluid	Cycle	Net power output	Working fluid pump power	Pump outlet pressure	Working fluid mass flow	Expander volume flow (out)	Expander efficiency	Heat source outlet temperature
		kW	kW	bar	kg/s	m³/s	-	°C
R134a	RC	93	22.1	38.6	5.3	0.16	0.80	45.1
	TFC	61	38.5	38.6	9.3	0.18	0.72	34.7
R245fa	RC	90	4.6	12.1	3.7	0.45	0.80	63.5
	TFC	91	18.7	29.4	5.7	0.49	0.74	52.1
R1234ze(E)	RC	96	21.1	34.5	5.3	0.20	0.80	48.2
	TFC	73	34.4	34.5	8.6	0.23	0.74	35.7
Butane	RC	89	6.5	14.7	1.9	0.33	0.80	64.0
	TFC	90	23.8	32.8	2.8	0.35	0.74	53.8
Isopentane	RC	87	2.7	6.5	1.9	0.71	0.80	64.9
	TFC	90	13.2	15.9	3.4	0.85	0.71	49.8
Propane	RC	88	23.6	40.4	2.4	0.13	0.80	50.0
	TFC	48	49.8	40.4	5.1	0.15	0.70	35.1

DOI: 10.18462/iir.gl.2018.1286

Table 5. Selected result details. Case III (200°C) with 1500 m².

Fluid	Cycle	Net power output	Working fluid pump power	Pump outlet pressure	Working fluid mass flow	Expander volume flow (out)	Expander efficiency	Heat source outlet temperature
		kW	kW	bar	kg/s	m³/s	-	°C
R134a	RC	164	25.6	38.6	6.1	0.24	0.80	39.7
	TFC	91	56.9	38.6	13.7	0.27	0.72	29.6
R245fa	RC	208	24.3	34.7	6.2	0.75	0.80	44.8
	TFC	181	33.4	34.7	8.5	0.84	0.76	33.2
R1234ze(E)	RC	168	26.8	34.5	6.7	0.30	0.80	38.6
	TFC	109	51.1	34.5	12.8	0.35	0.74	29.7
Butane	RC	206	30.3	36.1	3.3	0.56	0.80	44.1
	TFC	175	41.7	36.1	4.5	0.63	0.76	33.2
Isopentane	RC	187	9.6	14.2	2.8	1.10	0.80	60.0
	TFC	213	27.8	32.1	3.5	1.22	0.78	45.5
Propane	RC	153	31.2	40.4	3.2	0.20	0.80	39.8
	TFC	71	73.6	40.4	7.5	0.23	0.70	30.0

Adding a recuperator can increase the efficiency of a power cycle and is thus favorable from a thermodynamic point of view. However, it adds cost and complexity to the system, so it should only be included when economically reasonable. Some of the optimized cycles showed an available temperature difference for recuperation of 60 K. However, when a recuperator was added, this difference decreased as the area for the recuperator was deducted from the other heat exchangers. Therefore, the net power output could not be increased significantly for any of the cycles and the detailed results were not included in this article.

4. DISCUSSION AND CONCLUSIONS

RC and the TFC were compared for power production from low temperature heat sources with six different working fluids. The calculated performances differed at a heat source inlet temperature of 100°C, but were similar for 150°C and 200°C inlet temperature. However, the TFC required significantly higher expander outlet volume flows, indicating a larger and more expensive system. The outlet pressure of the working fluid pump was also generally higher for the TFC.

The total efficiency of the TFC expander was calculated based on simple correlations. The average efficiency across all cases was 0.71 with a maximum of 0.784. The isentropic efficiency of the RC expander was assumed constant in this study. Due to the high maturity of this technology, a value of 0.80 was chosen. Thus, the TFC had a lower expander efficiency than the RC, which was the main cause why the presented results deviate from other studies (e.g. Zamfirescu and Dincer (2008), Fischer (2011), Lai and Fischer (2012), Chan *et al.* (2013)) by being less promising for the TFC. However, a more detailed and verified calculation method for the expander efficiency in both RC and TFC is required for a fully realistic comparison.

The natural working fluids showed similar performance to the conventional refrigerants, indicating that hydrocarbons could provide environmentally friendly alternatives to the standard systems used today. R1234z(E) was also found to be a suitable working fluid with low environmental impact. It could be shown that the critical temperature is an important parameter for the working fluid choice in a TFC. A high difference between heat source inlet temperature and critical temperature of the working fluid led to poor temperature matching in the heat recovery heat exchanger and thus to low performance. The pinch point in the heat recovery heat exchanger limited the performance of the RC as it prevented reasonable use of more heat exchanger area.

NOMENCLATURE

P	Work (W)	U	Heat transfer coefficient ($W \cdot m^{-2} \cdot K^{-1}$)
η	Efficiency (-)	LMTD	Log mean temperature difference (K)

DOI: 10.18462/iir.gl.2018.1286

A	Area (m²)	ρ	Vapor density (kg·m^{-3})
Q	Heat flow (W)	q	Vapor quality (-)

REFERENCES

Bao, J. and Zhao, L., 2013. A review of working fluid and expander selections for organic Rankine cycle. Renewable and Sustainable Energy Reviews 24(0), 325-342.
Brown, B.W. and Mines, G.L., 1998. Flowsheet Simulation of the Trilateral Cycle. Geothermal Resources Council Transactions 22, 373-377.
Chan, C.W., Ling-Chin, J. and Roskilly, A.P., 2013. A review of chemical heat pumps, thermodynamic cycles and thermal energy storage technologies for low grade heat utilisation. Appl Therm Eng 50(1), 1257-1273.
DiPippo, R., 2007. Ideal thermal efficiency for geothermal binary plants. Geothermics 36(3), 276-285.
Fischer, J., 2011. Comparison of trilateral cycles and organic Rankine cycles. Energy 36(10), 6208-6219.
Galanis, N., Cayer, E., Roy, P., Denis, E.S. and Désilets, M., 2009. Electricity Generation from Low Temperature Sources. Journal of Applied Fluid Mechanics 2, 55-67.
Hays, L., 2010. Demonstration of a Variable PhaseTurbine Power System for Low Temperature Geothermal Resources. U.S. Department of Energy. Geothermal Technologies Program. Report Number G015153.
Ho, T., 2012. Advanced Organic Vapor Cycles for Improving Thermal Conversion Efficiency in Renewable Energy Systems. PhD Thesis, University of California, Berkeley.
Hu, L., Wang, Z., Fan, W., Pang, F. and Lu, C., 1989. An organic total flow system for geothermal energy and waste heat conversion. 24th Intersociety Energy Conversion Engineering Conference, Wash. DC, USA.
Lai, N.A. and Fischer, J., 2012. Efficiencies of power flash cycles. Energy 44(1), 1017-1027.
Lemmon, E.W., Huber, M.L. and McLinden, M.O., 2013. National Institute of Standards and Technology. Reference Fluid Thermodynamic and Transport Properties - REFPROP, Version 9.1.
Li, J., Liu, Q., Ge, Z., Duan, Y. and Yang, Z., 2017. Thermodynamic performance analyses and optimization of subcritical and transcritical organic Rankine cycles using R1234ze(E) for 100–200°C heat sources. Energy Conversion and Management 149(Supplement C), 140-154.
Quoilin, S., Broek, M.V.D., Declaye, S., Dewallef, P. and Lemort, V., 2013. Techno-economic survey of Organic Rankine Cycle (ORC) systems. Renewable and Sustainable Energy Reviews 22(0), 168-186.
Quoilin, S., Declaye, S., Tchanche, B.F. and Lemort, V., 2011. Thermo-economic optimization of waste heat recovery Organic Rankine Cycles. Applied Thermal Engineering 31(14–15), 2885-2893.
Smith, I.K., 1993. Development of the Trilateral Flash Cycle System: Part 1: Fundamental Considerations. P I Mech Eng, Part A: Journal of Power and Energy 207, 179-194.
Smith, I.K., Stosic, N. and Aldis, C., 1994. Lysholm Machines as Two-Phase Expanders. International Compressor Engineering Conference, Purdue University, Indiana, USA.
Smith, I.K., Stosic, N. and Aldis, C., 1995. Trilateral Flash Cycle System: A High Efficiency Power Plant for Liquid Resources. World Geothermal Congress, Florence, Italy.
Smith, I.K., Stosic, N. and Kovacevic, A., 2005. Screw Expanders Increase Output and Decrease the Cost of Geothermal Binary Power Plant Systems. Geothermal Resources Council Transactions 29, 787-794.
Steffen, M., Löffler, M. and Schaber, K., 2013. Efficiency of a new Triangle Cycle with flash evaporation in a piston engine. Energy 57(0), 295-307.
Trædal, S., Rohde, D. and Eikevik, T.M., 2014. Analysis of the Trilateral Flash Cycle and the Partially Evaporating Cycle for power production from low temperature heat sources. 11th IIR Gustav Lorentzen Conference, Hangzhou, China.
Welch, P. and Boyle, P., 2009. New Turbines to Enable Efficient Geothermal Power Plants. Geothermal Resources Council Transactions 33, 765-772.
Yari, M., Mehr, A.S., Zare, V., Mahmoudi, S.M.S. and Rosen, M.A., 2015. Exergoeconomic comparison of TLC (trilateral Rankine cycle), ORC (organic Rankine cycle) and Kalina cycle using a low grade heat source. Energy 83, 712-722.
Zamfirescu, C. and Dincer, I., 2008. Thermodynamic analysis of a novel ammonia–water trilateral Rankine cycle. Thermochimica Acta 477(1-2), 7-15.
Zyhowski, G. and Brown, A., 2011. Low Global Warming Fluids for Replacement of HFC-245fa and HFC-134a in ORC Applications. First International Seminar on ORC Power Systems, Delft, The Netherlands.